

Timelike geodesics of a modified gravity black hole immersed in an axially symmetric magnetic field

Saqib Hussain^{1,*} and Mubasher Jamil^{2,†}

¹*Department of Physics, School of Natural Sciences (SNS),
National University of Sciences and Technology (NUST), H-12, Islamabad, Pakistan*

²*Department of Mathematics, School of Natural Sciences (SNS),
National University of Sciences and Technology (NUST), H-12, Islamabad, Pakistan*

Abstract: We investigate the dynamics of a neutral and a charged particle around a black hole in modified gravity immersed in magnetic field. Our focus is on the scalar-tensor-vector theory as modified gravity. We are interested to explore the conditions on the energy of the particle under which it can escape to infinity after collision with another neutral particle in the vicinity of the black hole. We calculate escape velocity of particle orbiting in the innermost stable circular orbit (ISCO) after the collision. We study the effects of modified gravity on the dynamics of particles. Further we discuss how the presence of magnetic field in the vicinity of black hole, effects the motion of the orbiting particle. We show that the stability of ISCO increases due to presence of magnetic field. It is observed that a particle can go arbitrary close to the black hole due to presence of magnetic field. Furthermore ISCO for black hole is more stable as compared with Schwarzschild black hole. We also discuss the Lyapunov exponent and the effective force acting on the particle in the presence of magnetic field.

*Electronic address: s.hussain2907@gmail.com

†Electronic address: mjamil@sns.nust.edu.pk; jamil.camp@gmail.com

I. INTRODUCTION

Theories of modified gravity (such as $f(R)$ theory, Lovelock gravity, Gauss-Bonnet theory etc) are constructed by adding curvature correction terms in the usual Einstein-Hilbert action through which the cosmic accelerated expansion might be explained [1] (see also [2] for reviews on modified gravity). Such correction terms give rise to solutions of the field equations without invoking the concept of dark energy. To find the dynamical equations one can vary the action according to the metric. There is no restriction on the gravitational Lagrangian to be a linear function of Ricci scalar R [3]. Recently some authors have taken into serious consideration the Lagrangians that are “stochastic” functions with the requirement that it should be local gauge invariant [4]. This mechanism was adopted in order to treat the quantization on curved spacetime. The result was that corrective term in the Einstein Hilbert Lagrangian arises due to either background geometry and interactions among quantum fields or gravitational self interaction [5]. Furthermore, it is also realized that such corrective terms should be incorporated if one wants to obtain the effective action of quantum gravity on Planck scale [6]. Besides fundamental physical motivation, these theories have acquired a huge interest in cosmology as they exhibit inflationary behaviors and that the corresponding cosmological model seem very realistic [7, 8]. In this article, our focus will be on the scalar-tensor-vector theory (will be referred as MOG) and the Schwarzschild-MOG black hole (MOG) [9].

Black holes can accelerate particles to arbitrarily high energy if the angular momentum of the particle is fine-tuned to some critical value (see [10] and references therein). This phenomenon is robust as it is founded on the basic properties of geodesics around a black hole [11]. Studying the dynamics of a particle (either massive or massless) around the gravitational source such as a black hole (BH) is important because it is responsible for understanding the geometrical structure of spacetime near the BH. Geodesics may display a rich structure and convey a very reliable information to understand the geometry of the BH. There are many types of geodesic motion but the circular geodesics are specially important. The exponential fade-out of a collapsing star’s luminosity can be explained by the circular geodesics as given in [12, 13]. The motion of test particles helps to study the gravitational fields of objects experimentally and to compare the observations with the predictions about observable effects (light deflection, gravitational time delay and perihelion shift).

In the surrounding of the BH, a magnetic field is generally present [14], due to the presence of plasma in the vicinity of the BH. The accretion disk or a charged gas cloud is primarily responsible

for the magnetic field field [15, 16]. The magnetic field is stronger in the vicinity of BH's event horizon however it does not effect the geometry of the BH, but the motion of the charged particle moving around a BH is effected [17, 18]. The magnetic coupling process is likely responsible for the stability of black hole with its accretion disc [19]. According to this process, angular momentum and energy are transferred from the black hole to its surrounding disc. The magnetic field plays an important role in transferring sufficient energy to the surrounding particles for escaping to spacial infinity [20, 21]. Other interesting processes around BHs include evaporation and phantom energy accretion onto BHs [22]. In this article, we revisit the model of Zahrani et al [23] for a MOG black hole and explore the effects of modified gravity. It involves the collision of a bounded particle with an unbounded particle in the vicinity of the black hole. The main interest lies in finding the conditions of escape of a bounded particle after the collision.

The outline of the paper is as follows: In section II we develop the basic equations and then derive an expression for escape velocity of a neutral particle. In section III we discuss the strength of magnetic field, and the equations of motion of the charged particle moving around weakly magnetized MOG and escape velocity for particle also calculated. Force acting on the particle is studied in section IV and geodesics of the particles moving around the MOG are discuss in section V. Lyapunov exponent is explained in section VI. In section VII and VIII, trajectories for effective potential and escape velocity of the particle are presented respectively. Conclusion is given in last section. We will study the motion of particle in the equatorial plane to simplify the calculations. Throughout this work we use the following metric signature $(+, -, -, -)$ and assume $c = 1$.

II. NEUTRAL PARTICLE DYNAMICS AROUND MOG BLACK HOLE

Motion of particles around a central massive object under the affect of a central force is a well-studied problem of classical mechanics (or rather Newtonian mechanics). In particular we can think of the following problem in the present context: consider a particle of mass m moving in a circular orbit around another object of mass M such that $M \gg m$. Now for the particle to escape from the gravitational field of M , particle's initial velocity must be more than the escape velocity. The particle can gain the escape velocity either from an external force acting on it or by hitting (or colliding) a test particle with the particle in circular orbit. Since the collision leads to transfer of energy as well, the particle will escape from the circular orbit if its energy after collision is more than a critical energy or escape energy. If however, the energy of the particle after collision is small than the critical energy, the particle falls towards M .

The relativistic version of the above scenario was investigated by Zahrani et al [23]. They studied the motion of a charged particle in the vicinity of a weakly magnetized Schwarzschild black hole and focused on the bounded trajectory lying in the black hole equatorial plane. For the charged particle to escape from the innermost circular orbit, another particle (which is neutral and coming from sufficiently far distance) hits the charged particle. The authors obtained the corresponding conditions of escape velocity and escape energy in the resulting process. They also predicted that the motion of charged particle after collision will be chaotic due to the presence of magnetic field and strong gravitational field. Although the chances of collision between two particles around black hole, in general are feeble. However the process itself is important to describe the ejection of particles from the vicinity of black holes. Later on Hussain et al [24] investigated a similar scenario for a slowly rotating Kerr black hole and discussed the conditions of escape for the particle. Jamil et al [25] investigated a similar scenario for a Schwarzschild black hole surrounded by quintessence.

Recently, Moffat [9] obtained both static and non-static black hole solutions in the scalar-tensor-vector modified gravity, the theory which he himself proposed [26]. The theory fairly describes several astronomical and cosmological observations such as galaxy rotation curves [27] and gravitational lensing [28]. The modified gravitational field equations are given by [9, 26]:

$$R_{\mu\nu} - \frac{1}{2}g_{\mu\nu}R = -8\pi GT_{\mu\nu}^{\varphi}, \quad (1)$$

where

$$T_{\mu\nu}^{\varphi} = -\frac{1}{4\pi} \left(B_{\mu}^{\sigma} B_{\nu\sigma} - \frac{1}{4} g_{\mu\nu} B^{\sigma\beta} B_{\sigma\beta} \right),$$

and $B_{\mu\nu} = \varphi_{\nu,\mu} - \varphi_{\mu,\nu}$, where φ_{μ} is a vector field with the source charge $Q = \sqrt{\alpha G_N} M$ (see details below). The role of this vector field is to produce large scale repulsive gravity which can cause accelerated cosmic expansion. Further the vacuum field equations are

$$B^{\mu\nu}{}_{;\nu} = 0, \quad B_{[\mu\nu;\sigma]} = 0 \quad (2)$$

where $;$ denotes the covariant derivative operation.

To solve the above system of equations, an ansatz for the static and spherically symmetric solution is assumed of the form

$$ds^2 = g(r)dt^2 - g(r)^{-1}dr^2 - r^2(d\theta^2 + \sin^2\theta d\phi^2). \quad (3)$$

The calculation yields [9]

$$g(r) = 1 - 2\frac{GM}{r} + \alpha\frac{G_N GM^2}{r^2},$$

$$G = G_N(1 + \alpha), \quad Q = \kappa M, \quad \kappa = \pm\sqrt{\alpha G_N}, \quad \alpha = \frac{G}{G_N} - 1, \quad (4)$$

and therefore we have

$$Q = \pm \sqrt{\alpha G_N M}. \quad (5)$$

Note that α is a free parameter of the theory, hence it yields a variable gravitational *constant*. Here M and Q is respectively mass and electric charge of the black hole and G_N is the Newton's gravitational constant. In metric (3), positive value of Q is chosen to maintain repulsive gravitational force as it is necessary to describe the stable star. (For a stable star, the gravitational attraction should be balanced by the repulsive gravity). This is a static, spherically symmetric, point particle solution of a electrically charged body like Reissner-Nordstrom black hole [31, 32]. For $\alpha = 0$, metric (3) reduces to the Schwarzschild metric (which is also the general relativistic limit). Like Kerr [33] and Reissner Nordstörn metrics it has two horizons:

$$r_{\pm} = G_N M \left(1 + \alpha \pm (1 + \alpha)^{\frac{1}{2}} \right). \quad (6)$$

Eq. (6) corresponds to $g(r) = 0$ and will reduce to Schwarzschild event horizon for $\alpha = 0$. The metric (3) is invariant under time translation and rotation around symmetry axis. Thus the Killing vectors equations are [34]:

$$\xi_{(t)}^{\mu} \partial_{\mu} = \partial_t, \quad \xi_{(\phi)}^{\mu} \partial_{\mu} = \partial_{\phi}, \quad (7)$$

which will give the constants of motion, where $\xi_{(t)}^{\mu} = (1, 0, 0, 0)$ and $\xi_{(\phi)}^{\mu} = (0, 0, 0, 1)$. The conserved quantities corresponding to these Killing vectors are the total energy (per unit mass) \mathcal{E} and azimuthal angular momentum L_z (per unit mass) of the moving particle at infinity. Motion of a neutral particle moving in MOG background is described by the Lagrangian density [35],

$$\mathcal{L} = \frac{1}{2} g_{\mu\nu} \dot{x}^{\mu} \dot{x}^{\nu}. \quad (8)$$

From (4) and (8) we can say that t and ϕ are the cyclic coordinates. There exists constants of motion corresponding to these cyclic coordinates i.e. total energy and azimuthal angular momentum. We have calculated these integral of motion by using the Euler-Lagrange equation

$$\frac{d}{d\tau} \left(\frac{\partial \mathcal{L}}{\partial \dot{x}^{\mu}} \right) - \frac{\partial \mathcal{L}}{\partial x^{\mu}} = 0. \quad (9)$$

Therefore, using equation (9) for t and ϕ we have

$$\frac{dt}{d\tau} = \dot{t} = \frac{\mathcal{E}}{g(r)}, \quad (10)$$

$$\frac{d\phi}{d\tau} = \dot{\phi} = -\frac{L_z}{r^2}. \quad (11)$$

The over dot denotes the differentiation with respect to proper time τ throughout the calculations. Considering the planar motion of the particle i.e. for $\theta = \pi/2$ the normalization condition $u^\mu u_\mu = 1$, gives

$$\begin{aligned} \dot{r}^2 &= \mathcal{E}^2 - U_{\text{eff}}, \\ U_{\text{eff}} &= \left(1 - 2\frac{GM}{r} + \alpha\frac{G_N GM^2}{r^2}\right)\left(1 + \frac{L_z^2}{r^2}\right). \end{aligned} \quad (12)$$

The extreme values of the effective potential correspond to $\frac{dU_{\text{eff}}}{dr} = 0$. It occurs at $r = 6M$ for a Schwarzschild black hole [23]. The point where the ISCO exists is the convolution point of the effective potential [36]. In the present case, the ISCO occurs at

$$\begin{aligned} r_o &= \frac{\alpha GM^2 G_N + L^2}{3GM} - \left(\sqrt[3]{2} (L(L - 3GM) + \alpha GM^2 G_N) (L(3GM + L) + \alpha GM^2 G_N) \right) \\ &\quad \left[3GM \left(-2\alpha^3 G^3 M^6 G_N^3 + 3GL^4 M^2 (9G - 2\alpha G_N) - 2L^6 - 3\alpha G^2 L^2 M^4 G_N (2\alpha G_N + 9G) \right. \right. \\ &\quad \left. \left. + 3\sqrt{3} \left(G^3 L^2 M^4 \left(-9GL^6 + 108G^3 L^4 M^2 + \alpha G_N (8L^6 - 126G^2 L^4 M^2 \right. \right. \right. \right. \\ &\quad \left. \left. \left. + \alpha GM^2 G_N (24L^4 - 9G^2 L^2 M^2 + 8\alpha GM^2 G_N (\alpha GM^2 G_N + 3L^2)) \right) \right) \right)^{\frac{1}{2}} \right]^{\frac{1}{3}} - 1 \\ &\quad - \frac{1}{3\sqrt[3]{2}GM} \left(-2\alpha^3 G^3 M^6 G_N^3 + 3GL^4 M^2 (9G - 2\alpha G_N) - 2L^6 - 3\alpha G^2 L^2 M^4 G_n (2\alpha G_N + 9G) \right. \\ &\quad \left. + 3\sqrt{3} \left(G^3 L^2 M^4 \left(-9GL^6 + 108G^3 L^4 M^2 + \alpha G_N (8L^6 - 126G^2 L^4 M^2 \right. \right. \right. \right. \\ &\quad \left. \left. \left. + \alpha GM^2 G_N (24L^4 - 9G^2 L^2 M^2 + 8\alpha GM^2 G_N (\alpha GM^2 G_N + 3L^2)) \right) \right) \right)^{\frac{1}{2}} \right]^{\frac{1}{3}} \end{aligned} \quad (13)$$

The critical energy and the azimuthal angular momentum of the particle corresponding to ISCO are

$$\mathcal{E}_o = \frac{(\alpha GM^2 G_N + r(r - 2GM))^2}{r^2 (2\alpha GM^2 G_N + r(r - 3GM))}, \quad (14)$$

$$\mathcal{L}_{zo} = \frac{\sqrt{GM r^3 - \alpha GM^2 r^2 G_N}}{\sqrt{2\alpha GM^2 G_N - 3GM r + r^2}}. \quad (15)$$

We consider the case that an incoming particle collides with the orbiting particle at the ISCO, so that after collision it will move within a new plane tilted with respect to previous equatorial plane. However, to study the dynamics of a particle it is convenient to use the fact that if the initial position and the tangent vector of the trajectory of the particle lies on a plane that contain the center of the body, then the entire trajectory lies on this plane. After collision, there are

three possible cases depending on the collision mechanism : (i) bound motion (ii) capture by BH (iii) escape to infinity. For a little change in energy and angular momentum, orbit of the particle alters very slightly. While for large changes it may escape to infinity or capture by BH depending upon the nature of change in path. After collision, the particle will no longer remain in the same equatorial plane, so further discussion would be dealt with respect to new plane. But note that due to spherical symmetry all equatorial planes are equivalent. Due to collision particle should have new constants of motion \mathcal{E} , L^2 and L_z . For simplification of our problem we consider the case of collision when (i) the azimuthal angular momentum is invariant during collision (ii) initial radial velocity does not change. These conditions imply that only energy of the particle will change hence its motion would be determined by considering only the change in the energy. After collision particle acquires an escape velocity v , in orthogonal direction of the equatorial plane as explained in [14]. The angular momentum and energy of the particle after collision becomes (at the equatorial plan $\theta = \frac{\pi}{2}$)

$$L^2 = r_o^2 v^2 + \frac{L_{zo}^2}{\sin^2 \theta}, \quad L^2 = r_o^2 v^2 + L_{zo}^2 \quad (16)$$

Here $v \equiv -r_o \dot{\theta}_o$ and $\dot{\theta}_o$ is the initial polar angular velocity of the particle and r_o is the radius of ISCO. This velocity should be in orthogonal direction to the equatorial plane [37]. Further

$$\mathcal{E} = \sqrt{\left(1 - \frac{2GM}{r} + \frac{\alpha G_N G M^2}{r^2}\right) v^2 + \mathcal{E}_o^2}, \quad (17)$$

where \mathcal{E}_o is defined in Eq. (14). It is clear that these values of angular momentum (16) and energy (17) are larger than their values (14) and (15) before collision. Also Eq. (17) shows that as $r \rightarrow \infty$, $\mathcal{E} \rightarrow \mathcal{E}_o \rightarrow 1$. So for $\mathcal{E} \equiv \mathcal{E} \geq 1$ particle will have unbound motion. In other words the particle can not escape to infinity if $\mathcal{E} < 1$. Hence the necessary condition for a particle to escape to infinity after collision is $\mathcal{E} \geq 1$ or

$$v \geq \frac{\sqrt{r(2GM(L^2 + r^2) - L^2 r) - \alpha G M^2 G_N (L^2 + r^2)}}{\sqrt{r^2(\alpha G M^2 G_N + r(r - 2GM))}}. \quad (18)$$

The last expression for velocity v is obtained by solving equation (17) at $\mathcal{E}_{\text{new}} = 1$.

III. MOTION OF A CHARGED PARTICLE AROUND A WEAKLY MAGNETIZED SMOG BLACK HOLE

A. Magnetic Field in the Vicinity of BH

The magnetic coupling (MC) process is responsible for attraction of black hole with its accretion disc [17, 19, 38–40]. According to this process angular momentum and energy are transferred from

a black hole to its surrounding disc. The process of MC provides the relation between the strength of magnetic field at the black hole horizon and its mass M and the rate of accretion \dot{M} [41]. This relation is as follows:

$$\mathcal{B}_h = \frac{1}{r_h} \sqrt{2m_p \dot{M} c}. \quad (19)$$

Here black hole horizon r_h is given by (6) and m_p is the magnetization parameter which indicates the relative power of process of MC with respect to disc accretion. If disc accretion dominant over MC process then $m_p < 1$ and if MC process is dominant over disc accretion then $m_p > 1$ while $m_p = 1$ correspond to equipartition of these two processes. The magnetic field expression is given by [41]

$$\mathcal{B}_h = \left(v_b f^2(\alpha, m_p) \right)^{\frac{1}{2}} \times 10^{7.35 + .45\theta}. \quad (20)$$

Magnetic field strength at the horizon of MOG-BH is 4.93×10^8 Gauss for $m_p = 1$, $\alpha = 0.1$, $\theta = 0.5$ and $v_b = 300$.

Similar effects of particle collision with high center of mass energy in the vicinity of black hole can also possible if the black hole is non rotating provided there exists a magnetic field in its surrounding. Since, there exists theoretical and experimental evidence that such a magnetic field should exist in the surrounding of black hole [21]-[29]. We assume that this magnetic field is weak and its energy and angular momentum does not effect the background geometry of the black hole. The above mentioned condition satisfy for a black hole of mass M if magnetic field strength holds the condition [30]

$$\mathcal{B} \ll \mathcal{B}_{max} = \frac{1}{G^{\frac{3}{2}} M_{\odot}} \left(\frac{M_{\odot}}{M} \right) \sim 10^{19} \frac{M_{\odot}}{M}. \quad (21)$$

These kind of black holes are called weakly magnetized.

B. Magnetic Field Calculation

In this section we explore how does the presence of a magnetic field in the BH exterior stimulate the motion of a charged particle. Firstly, we will calculate the magnetic field in the vicinity of black hole by following the procedure as given by [23, 24]

The Killing vector equation is [42]

$$\square \xi^{\mu} = 0, \quad (22)$$

where ξ^μ is a Killing vector. Eq. (22) corresponds to the Maxwell equation for 4-potential A^μ in the Lorentz gauge $A^\mu{}_{;\mu} = 0$. Defining A^μ as [43, 44]

$$A^\mu = \left(\frac{\alpha GM}{r}, 0, 0, \frac{\mathcal{B}}{2} \right). \quad (23)$$

Here magnetic field is defined as [23]

$$\mathcal{B}^\mu = -\frac{1}{2} e^{\mu\nu\lambda\sigma} F_{\lambda\sigma} u_\nu, \quad (24)$$

where

$$e^{\mu\nu\lambda\sigma} = \frac{\epsilon^{\mu\nu\lambda\sigma}}{\sqrt{-g}}, \quad \epsilon_{0123} = 1, \quad g = \det(g_{\mu\nu}). \quad (25)$$

Here $\epsilon^{\mu\nu\lambda\sigma}$ is the Levi Civita symbol, and $F_{\mu\nu}$ is the Maxwell tensor, defined as

$$F_{\mu\nu} = A_{\nu,\mu} - A_{\mu,\nu} = A_{\nu;\mu} - A_{\mu;\nu}. \quad (26)$$

For a local observer at rest, the component of four velocity are

$$u^\mu = (u^t, 0, 0, 0) = \left(g(r)^{-\frac{1}{2}}, 0, 0, 0 \right). \quad (27)$$

Here we assume $u^t > 0$, to signify the ‘forward-in-time’ condition. By equations (23-27) the magnetic field 4-vector becomes

$$\mathcal{B}^\mu = \left(0, \mathcal{B}g(r)^{\frac{1}{2}} \cos \theta, -\frac{\mathcal{B}g(r)^{\frac{1}{2}}}{r} \sin \theta, 0 \right). \quad (28)$$

The magnetic field is along with the z -axis at spatial infinity, and we assume that it is directed upward [45]. At equatorial plane only B^θ component will survive. In figure 1 we have plotted B^θ as a function of r . It is decreasing initially and then become almost constant for large r (away from the black hole). So, it is homogeneous at $r \rightarrow \infty$.

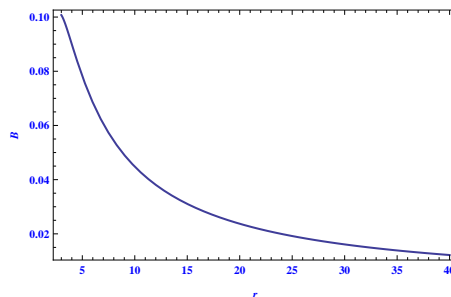


FIG. 1: In this figure we have plotted the magnetic field B^θ vs r for $\alpha = 0.2$.

C. Dynamical Equations

The Lagrangian of the moving particle of rest mass m and electric charge q in the vicinity of MOG-BH is

$$\mathcal{L} = \frac{1}{2}g_{\mu\nu}\dot{x}^\mu\dot{x}^\nu + \frac{q}{m}A_\mu\dot{x}^\mu. \quad (29)$$

Using Euler-Lagrange equation (27) for t and ϕ we get

$$g(r)\left(\dot{t} + \frac{\epsilon\alpha GM}{r}\right) = \mathcal{E}, \quad (30)$$

Here, $\epsilon = \frac{q}{m}$ is the specific charge of a particle and

$$\dot{\phi} = -\frac{L_z}{r^2 \sin^2 \theta} + B, \quad (31)$$

where

$$B \equiv \frac{\epsilon\mathcal{B}}{2}. \quad (32)$$

Using the normalization condition $u^\mu u_\mu = 1$, we obtain

$$1 = g(r)\dot{t}^2 - \frac{1}{g(r)}\dot{r}^2 - r^2\dot{\theta}^2 - r^2 \sin^2 \theta \dot{\phi}^2. \quad (33)$$

By using equations (30) and (31) in (33) and choosing $\theta = \frac{\pi}{2}$ we have

$$\dot{r}^2 + U_{\text{eff}} = \mathcal{E}^2, \quad (34)$$

and then effective potential is

$$\mathcal{E}_\pm = U_{\text{eff}\pm} = \frac{\epsilon GM}{r} \pm \sqrt{g(r)\left[1 + r^2\left(\frac{L_z}{r^2} - B\right)^2\right]}. \quad (35)$$

According to equation (16), after collision $L_z \rightarrow L$. Hence the effective potential reduces to

$$\mathcal{E}_\pm = U_{\text{eff}\pm} = \frac{\epsilon\alpha GM}{r} \pm \sqrt{g(r)\left[1 + r^2\left(\frac{L}{r^2} - B\right)^2\right]}. \quad (36)$$

Putting the value of L from equation (16) and $\mathcal{E}_\pm = 1$ in equation (36) and then solving for v we get

$$v = \frac{1}{r^4(\alpha GM^2 G_N + r(r - 2GM))} \left[GMr^2 (Br^2 - L) (\alpha MG_N - 2r) + Br^6 - Lr^4 \right. \\ \left. \pm \sqrt{GMr^6 (\alpha GM^2 G_N + r(r - 2GM)) (\alpha^2 GM \epsilon^2 - \alpha MG_N + r(2 - 2\alpha\epsilon))} \right]. \quad (37)$$

For a particle to escape from the black hole's vicinity, its velocity should be greater or equal to v .

A charged particle moving in an external electromagnetic field $F_{\mu\nu}$ obeys the equation of motion:

$$\ddot{x}^\mu + \Gamma_{\nu\sigma}^\mu \dot{x}^\nu \dot{x}^\sigma = \frac{q}{m} F_\alpha^\mu \dot{x}^\alpha. \quad (38)$$

The dynamical equations for θ and r respectively are

$$\ddot{\theta} = \frac{-2}{r} \dot{r} \dot{\theta} + \frac{L_z^2 \cos \theta}{r^4 \sin^3 \theta} - B^2 \sin \theta \cos \theta, \quad (39)$$

$$\begin{aligned} \ddot{r} = & \gamma - \dot{\theta}^2 \left(\gamma r^2 - r g(r) \right) - \frac{L^2}{r^2 \sin^2 \theta} \left(\gamma - \frac{g(r)}{r} \right) \\ & - B^2 \sin^2 \theta \left(-3r g(r) + r^2 \gamma \right) + BL \left(2\gamma - \frac{4g(r)}{r} \right), \end{aligned} \quad (40)$$

where $\gamma = \frac{M}{r^2} - \frac{\alpha GM^2}{r^3}$. For $\theta = \frac{\pi}{2}$ the equation (39) is satisfied obviously and equation (40) becomes

$$\ddot{r} = \gamma - \frac{L^2}{r^2} \left(\gamma - \frac{g(r)}{r} \right) - B^2 (-3r g(r) + r^2 \gamma) + BL \left(2\gamma - \frac{4g(r)}{r} \right). \quad (41)$$

We have solved equation (41) numerically by using the built in command of Mathematica NDSolve for $\alpha = 0.2$, $B = 0.3$ and $L_z = 2$ and plotted the solution in figure 2. In this figure the upper curve represents $r(\tau)$, middle is for \dot{r} (radial velocity) and the lower one is for \ddot{r} . \dot{r} is the radial velocity which represents the escape behavior as it is increasing with the increase of r , and \ddot{r} is the radial acceleration which is analogous to the force exerted on the particle in the radial direction after the collision.

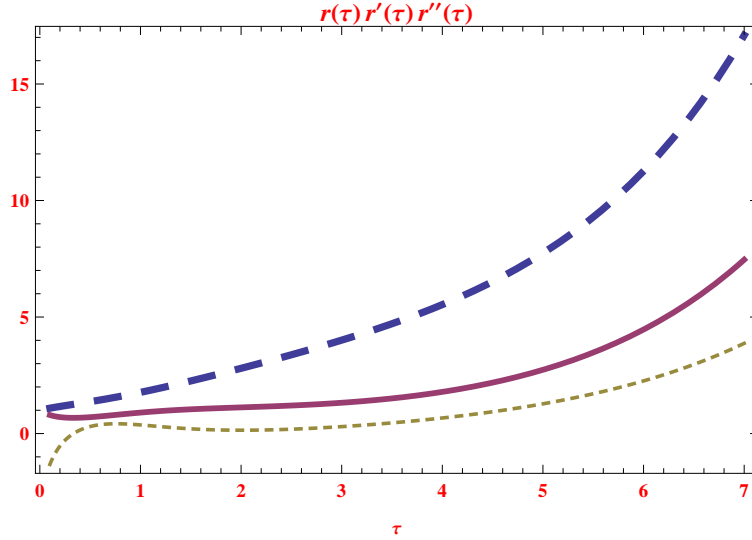


FIG. 2: Interpolating function $r(\tau)$ as the solution of Eq. (41) for $L_z = 2$, $B = 0.3$, and $\alpha = 0.2$. Here the large bold dashed curve represents $r\tau$, solid curve is for $\dot{r}(\tau)$ and Short dashed curve correspond to $\ddot{r}(\tau)$.

IV. FORCE ON A CHARGED PARTICLE IN THE VICINITY OF MOG-BH

As we have already calculated the effective potential for MOG-BH, we can also compute the effective force on a neutral and a charged particle by [46],

$$F = -\frac{1}{2} \frac{dU_{\text{eff}}}{dr}. \quad (42)$$

$$F = \frac{-G_N M (3L^2 + r^2) + L^2 r}{r^4} + \frac{\alpha G_N M ((\alpha + 1)G_N M (2L^2 + r^2) - r (3L^2 + r^2))}{r^5}. \quad (43)$$

It can be seen from equation (43) that the force due to scalar tensor-vector gravity is repulsive if $(\alpha + 1)G_N M (2L^2 + r^2) > -r (3L^2 + r^2)$.

$$F = \frac{L^2 r - GM (3L^2 + r^2)}{r^4} + \frac{Q^2 (2L^2 + r^2)}{r^5} \quad (44)$$

Equation (44) represents the effective force for RN-BH and the force due to charge of BH is repulsive with out any condition.

We are studying the dynamics of a neutral and a charged particle in the surrounding of MOG-BH where the scalar tensor-vector field produces a repulsive gravitational force which prevents a particle to fall into singularity [26]. In figure 3 we are comparing the effective force on a particle in the vicinity of MOG-BH with Schwarzschild black hole. We deduce from this figure that the repulsion to reach the singularity is more for $\alpha = 0.2$ as compared to $\alpha = 0$.

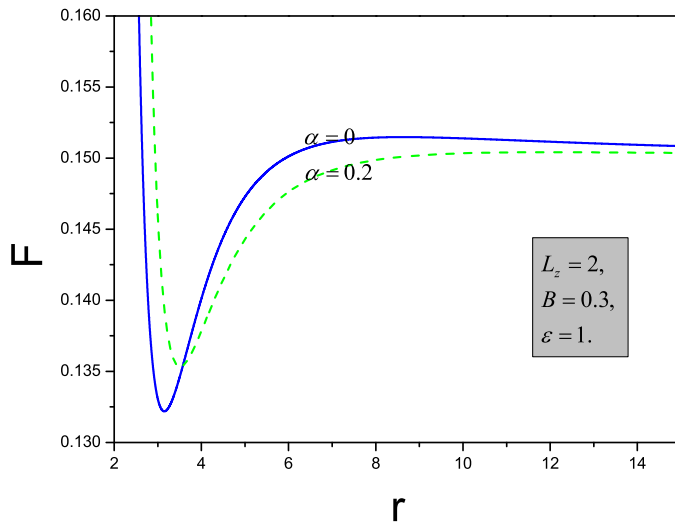


FIG. 3: Here we have plotted effective force as function of r for different values of α .

To study the behavior of force against magnetic field B we have plotted the force F as a function of r for different value of B in figure 4. It can be seen from this figure, due to large magnetic field strength B , force on the particle is more attractive as compared to small B .

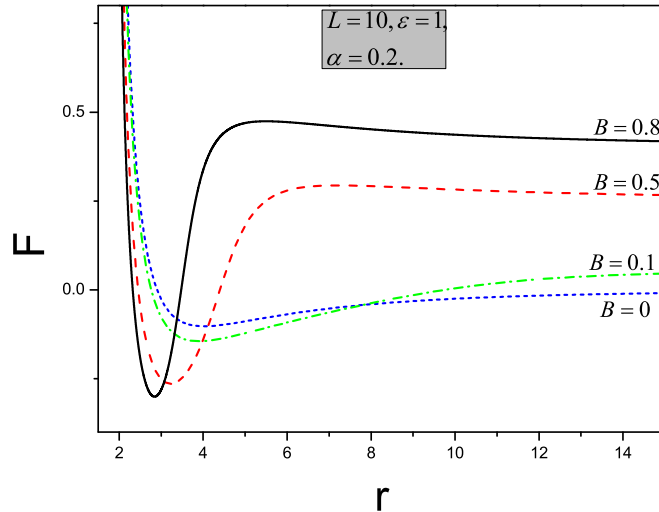


FIG. 4: Here we have plotted effective force against r for different values of magnetic field B .

V. COMPARISON OF GEODESICS IN THE VICINITY OF MOG-BH VS SBH

Geodesics of a Neutral Particle Moving Around a Schwarzschild BH:

Geodesics of a particle approaching toward or away from BH could be obtained by using Eqs. (10) and (12) together. We have:

$$\frac{dt}{dr} = \pm \frac{\mathcal{E}}{g(r)} \frac{1}{\sqrt{\mathcal{E}^2 - U_{\text{eff}}}}, \quad (45)$$

Here U_{eff} correspond to a neutral particle given by (12), where positive root gives the path of the particle out-going from the BH, and negative root gives the path of an ingoing particle. Let us consider the particle which is coming from infinity, initially at rest, approaches the BH, so setting $\mathcal{E} = 1$, $B = 0$, $\alpha = 0$ and $L_z = 2$ in Eq. (45) we plot the geodesics in (r, t) coordinates, see figure 5.

Geodesics of a Charged Particle Moving Around a MOG-BH:

Geodesics of the particles approaching the MOG-BH could be obtained by using Eqs. (30) and (34) together we obtain:

$$\frac{dt}{dr} = \pm \sqrt{\frac{\mathcal{E}g(r)^{-1} - \frac{\epsilon\alpha GM}{r}}{\mathcal{E}^2 - U_{\text{eff}}}}, \quad (46)$$

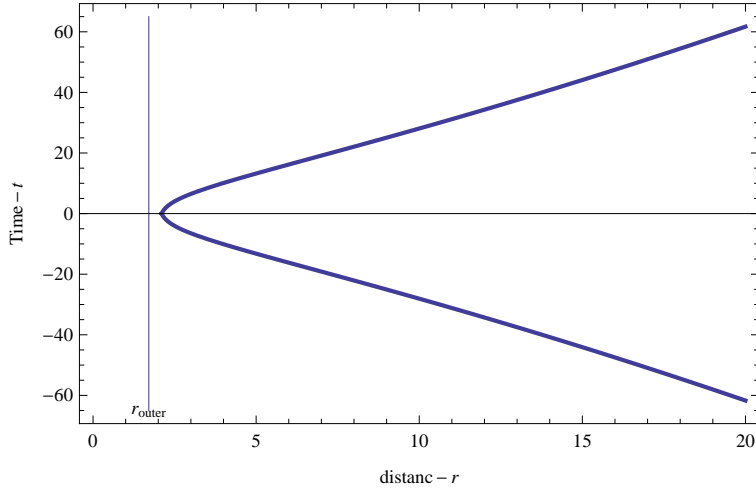


FIG. 5: Here we have plotted the geodesic equations $\frac{dt}{dr}$ (45) against r for $\mathcal{E} = 1$, $L_z = 2$, $M = 1$.

Here U_{eff} corresponds to a charged particle given by equation (36) where positive and negative signs give the path of the outgoing and ingoing particle respectively. Setting $\mathcal{E} = 1$, $L_z = 2$, $M = 1$, in Eq. (46) we get the geodesics which are bounded by the boundaries $r = r_c$ and the outer horizon of the BH, plotted in figure 6. In this figure, for thick curve we consider parameter $\alpha = 0.1$, magnetic field strength $B = 0.1$, and charge of a particle $\epsilon = 0.5$ and thin curve correspond to $\epsilon = 1$, $B = 0.5$ and $\alpha = 0.5$. Figure 6 shows that if the strength of magnetic field B is higher, then charged particle can reach arbitrary close to black hole as compared to smaller value of B .

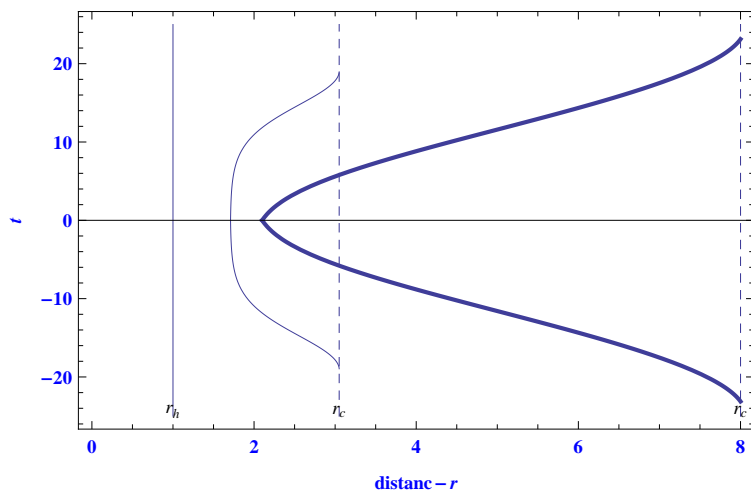


FIG. 6: Here we have plotted the geodesic equations $\frac{dt}{dr}$ (46) against r for $\mathcal{E} = 1$, $L_z = 2$, $M = 1$.

VI. STABILITY OF ORBITS

Lyapunov exponents are the measurements of the rate of convergence or divergence of the nearby trajectories in the phase space. It is highly sensitive to the initial conditions. Its positive value is the indication of divergence among the nearby trajectories. Therefore we can check the stability of orbits by the Lyapunov exponent λ [47]. It is given by

$$\lambda = \sqrt{\frac{-U''_{\text{eff}}(r_o)}{2\dot{t}(r_o)^2}}, \quad (47)$$

where r_o is the ISCO of the particle moving around BH. In [47] a critical component for the instability is defined as

$$\gamma = \frac{T_\lambda}{T}, \quad T_\lambda = \frac{1}{\lambda} \quad (48)$$

Here T_λ is the instability time scale. Time period for a circular orbits can be obtained from equation (11) in the absence of magnetic field as

$$T = \left| \frac{2\pi r_o^2}{L_z} \right|, \quad (49)$$

and in the presence of magnetic field, from equation (31) we have

$$T = \left| \frac{2\pi r_o^2}{-L_z + Br_o^2} \right| \quad (50)$$

Here r_o is the radius of circular orbit. We have plotted Lyapunov exponent as a function of magnetic field B in figure 7. It shows that the larger the magnetic field strength the lesser will be λ . From figure 7 and equation (50) one can say that the instability of circular orbits is more for a Schwarzschild black hole in comparison with the black hole immersed in a magnetic field. In figure 8 we have also plotted λ against α it decreases by the increase of α . Hence, the stability of circular orbits is less for the Schwarzschild black hole as compared to the black hole with non zero α .

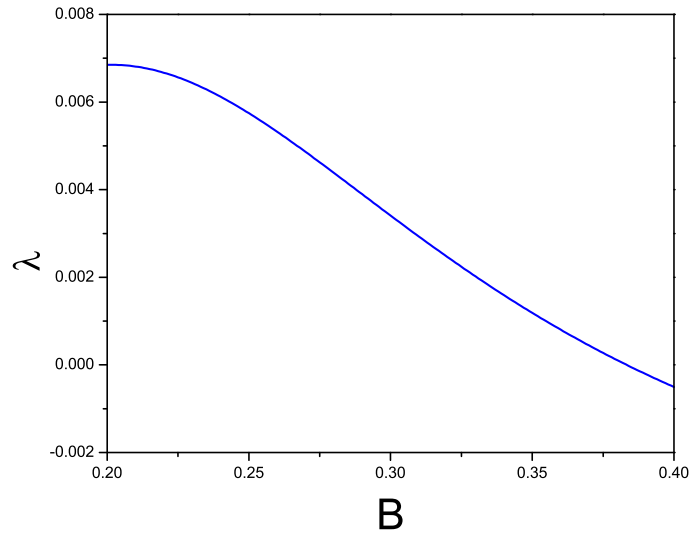


FIG. 7: In this figure we have plotted the Lyapunov exponent as a function of magnetic field B for $L = 6$, $\alpha = 0.5$, $\mathcal{E} = 1$, and $\epsilon = 1$.

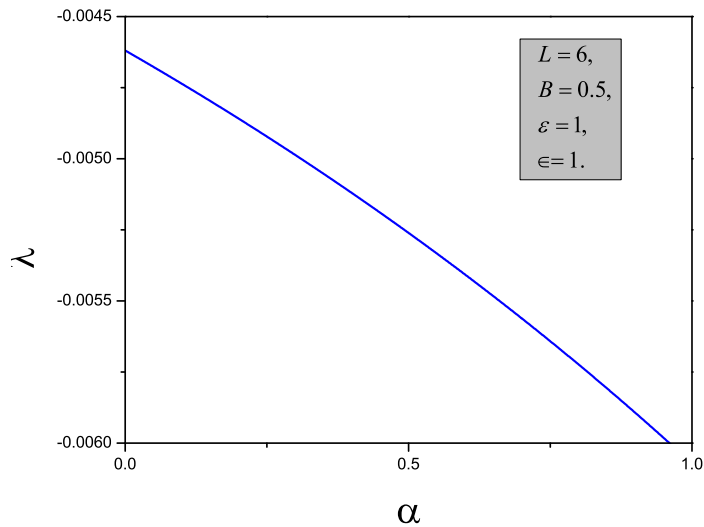


FIG. 8: Plotting of the Lyapunov exponent as a function of parameter α .

VII. BEHAVIOR OF EFFECTIVE POTENTIAL

Effective potential largely depends on g_{00} component of metric. Therefore, before discussing the behaviour of effective potential we will compare the g_{00} component of MOG-BH metric with RN-BH metric as it look similar. For RN-BH metric,

$$g_{00} = \left(1 - \frac{2M}{r} + \frac{Q^2}{r^2}\right), \quad (51)$$

for MOG-BH from equation (4) we have

$$g_{00} = \left(1 - \frac{2M}{r} - 2\sqrt{\alpha}\frac{Q}{r} + \sqrt{\alpha}(1 + \alpha)\frac{Q^2}{r^2} \right). \quad (52)$$

One can see that equation (51) contain only Q^2 term while equation (52) contain Q and Q^2 . This difference leads to large change between the behaviour of effective potential of these two black holes. The g_{00} component of MOG-BH metric also contain a parameter α which will create a main difference between the behaviour of potential.

In this section we plot the effective potential and graphically explain the conditions on the energy of the particle required for escape to infinity or for bound motion around MOG-BH. In figure 9 and figure 10 we have plotted U_{-eff} and U_{+eff} respectively correspond to equation (36). Here we will discuss the long distance and short distance behaviour of equation (36). One can see that for small value of r the square root term will dominate but for large r the term which is proportional to $\frac{1}{r}$ will dominate. For U_{+} we get some maximum value which we have mentioned in figure 10 as U_{max} . For a particle to fall into the black hole its energy should be greater then U_{max} otherwise it will bounce back to infinity or to some stable orbit. In case of U_{-} , particle can never cross the barrier as shown in the figure 9. Hence it cannot fall into the singularity.

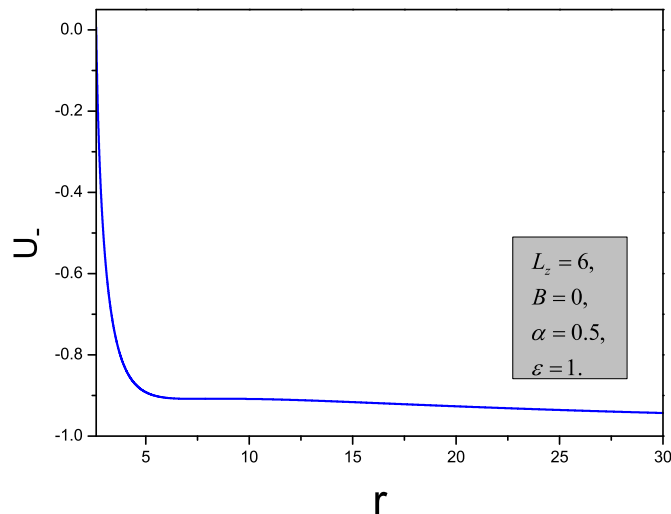


FIG. 9: In this figure we have plotted the effective potential U_{+} against radial coordinate r .

In figure 11 different regions of effective potential which correspond to escape and bound motion of the particle are shown. In figure 11, β corresponds to region of stable orbits. If the particle has energy equal or greater then δ , then it will fall into the black hole. U_{max} and U_{min} correspond to

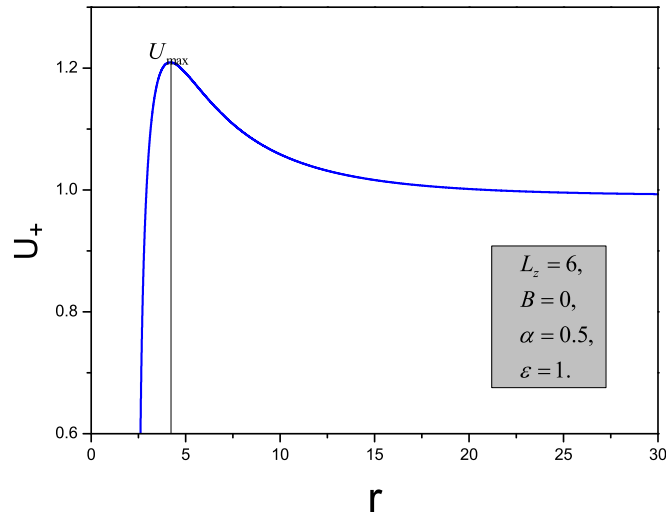


FIG. 10: In this figure we have plotted the effective potential U_+ as a function of r .

unstable and ISCO orbits respectively. If the energy of the the particle is equal or less than β then it will reside in one of the stable orbits. Particle having energy greater than β but less or equal to δ can have two possibilities: either it will escape to infinity or captured by the black hole. The local minima might be related to the change in behavior of the effective potential corresponds to BH (black brane transition) as observed in [48].

In figure 12 we are comparing the effective potential of Schwarzschild-BH, RN-BH and MOG-BH. It can be seen from this figure that for large r all the potentials approach to 1. Hence it can be concluded that the minimum energy required for a particle to escape from black hole vicinity is $\mathcal{E} = 1$ as we have mentioned before. Further the maxima for the effective potential of RN-BH is greater in comparison with the maxima of effective potential of Schwarzschild-BH and MOG-BH. Particle will be captured if it has energy greater than this maxima otherwise it will move back to infinity or may be reside in some stable orbit. Therefore, we can say that the possibility for a particle to escape from the vicinity of a black hole or to reside in some stable orbit is high in case of MOG-BH with $\alpha = 1.8$ in comparison to RN-BH and MOG-BH with $\alpha = 0.8$. Particle can reach to the singularity depending upon its energy, but it cannot reach the singularity for $\alpha = 1.8$ as shown by the curve, in figure 12. Note that $\alpha > 1$, corresponds to a naked singularity.

In figure 13 we are comparing the effective potentials in the presence with the absence of magnetic field. In this figure u_{max1} and u_{max2} correspond to unstable orbits while u_{min1} and u_{min2} is refers to ISCOs. One can notice that in the presence of magnetic field, minima of the effective potential is shifted towards the horizon and width of stable region is also increased in comparison

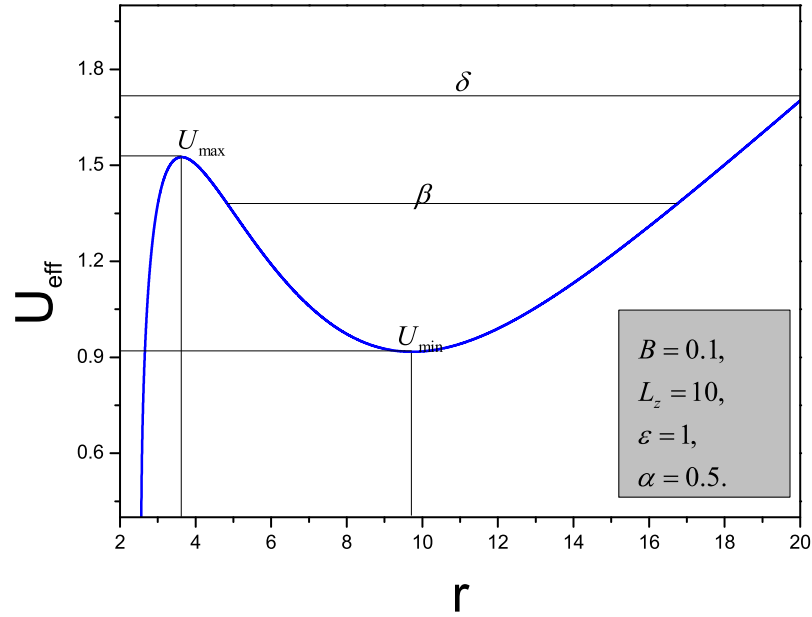


FIG. 11: In this figure different regions of effective potential which correspond to escape and bound motion of the particle are shown. Here β correspond to stable orbits for $b = 0.5$.

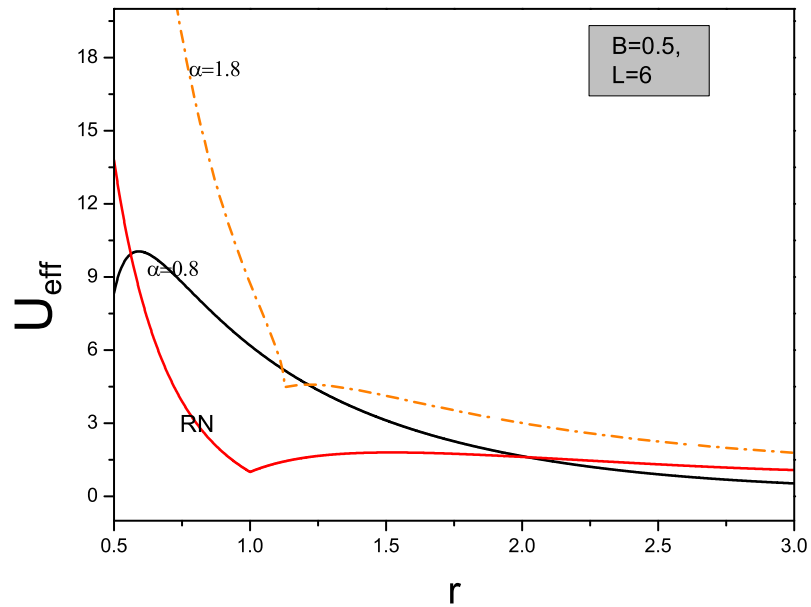


FIG. 12: Comparison of effective potential U_{eff} as a function of r . In this figure we are comparing the effective potential of RN-BH and MOG-BH.

with the case when the magnetic is absent. This is in agreement with [24, 44]. Therefore we can

say that magnetic field act as to increase the stability of the orbits.

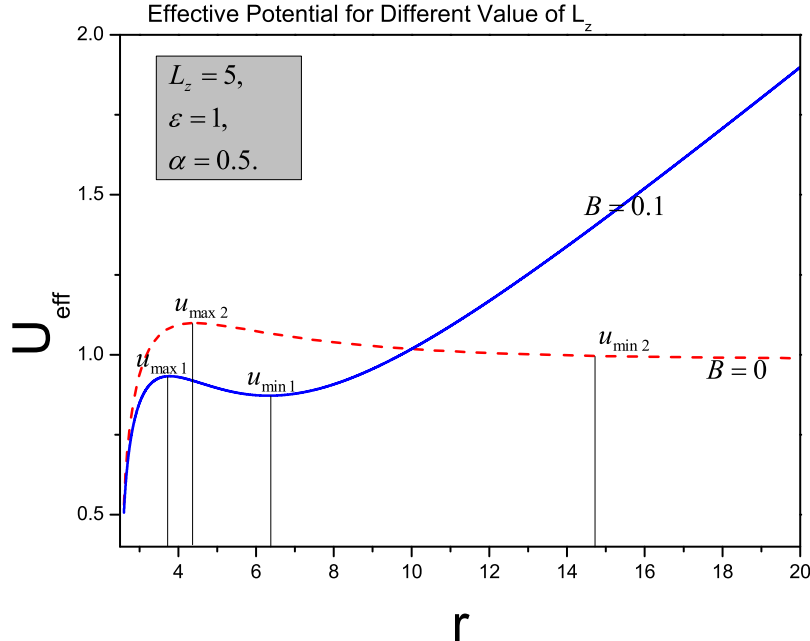


FIG. 13: Behavior of effective potentials with and without magnetic field versus r (a comparison).

In figure 14 we have plotted the effective potential as a function of r for different value of angular momentum L_z . One can see that for large value of L_z , the effective potential has local minima and maxima which correspond to stable and unstable circular orbits respectively. Hence we can say that the particle with greater value of L_z would have more possibility to reside in the stable orbits in comparison with lesser value of L_z .

To study the behaviour of effective potential against ϵ , we have plotted effective potential as a function of radial coordinate r for different values of ϵ in figure 15. It can be seen that larger the value of ϵ greater will be the maxima of potential. Therefore, large value of ϵ would correspond to easy escape and vice versa. It can be seen from the detailed analysis of the effective potential and the black hole physics that the scalar tensor-vector modified gravity differs from the Einstein's theory of gravity a lot at shorter distance and it becomes similar at long distance.

VIII. TRAJECTORIES OF ESCAPE VELOCITY

For the angular variable we have,

$$\frac{d\phi}{d\tau} = -\frac{L}{r^2} + B. \quad (53)$$

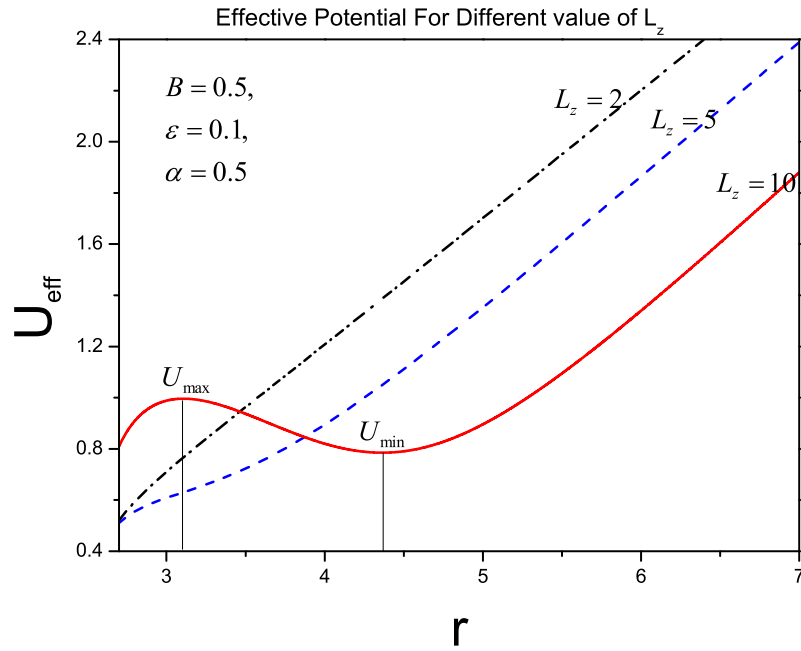


FIG. 14: Comparison of effective potentials with respect to L_z as a function of r .

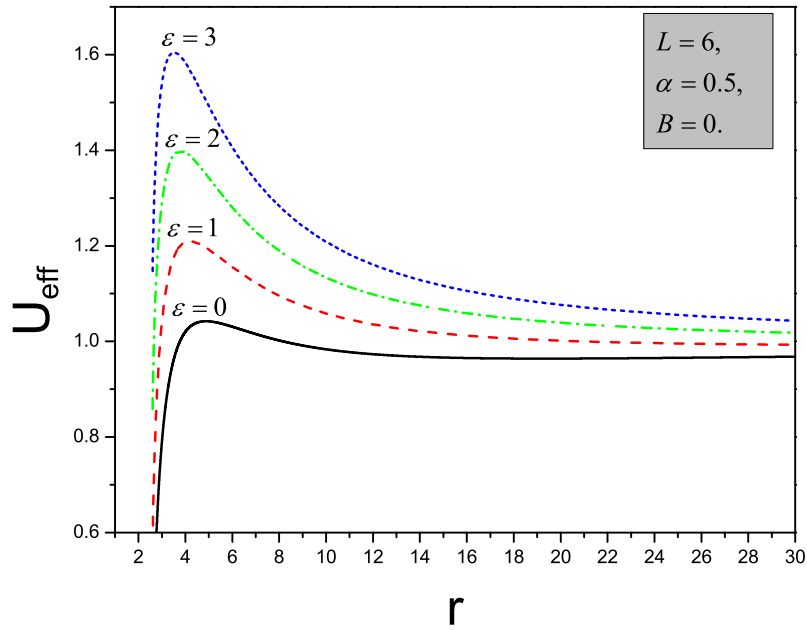


FIG. 15: Here we have plotted effective potential as function of r for different values of ϵ .

If the left hand side of equation (53) is negative then the Lorentz force on the particle is attractive [49]. The motion of the charged particle is in clockwise direction. Lorentz force is repulsive if left

hand side of (53) is positive. We are not going to the detail here because it is already discussed in [36, 49]. Our concern is only about the action of magnetic field on the charged particle. Therefore, magnetic field may deform the oscillatory motion, so, the greater the strength of magnetic field, the larger will be the deformation of the orbit. Hence we can conclude that larger the strength of magnetic field, easy for a particle to escape from the ISCO.

We have also plotted in figure 16 escape velocity as a function of radial coordinate for different values of magnetic field parameter b . It can be seen that the escape velocity of the particle increases as the magnetic field strength increases but it becomes almost constant just like magnetic field, away from the BH. As the magnetic field is strong near the BH, therefore, we can conclude that presence of magnetic field will provide more energy to particle, so that it might easily escape from the vicinity of BH. These conclusions are consistent with [15, 16].

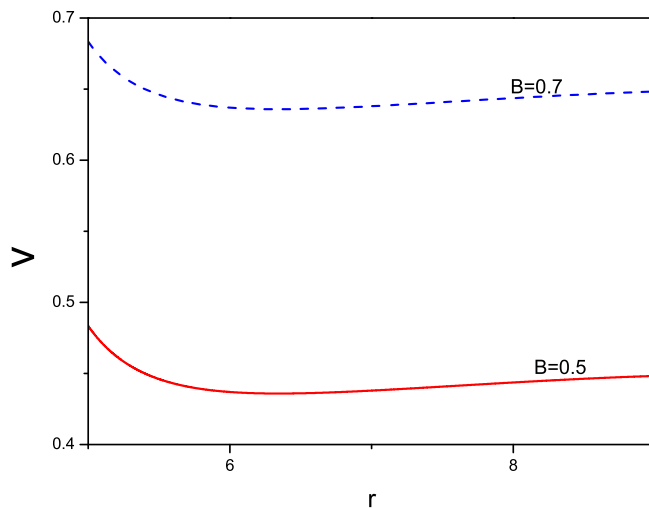


FIG. 16: Escape velocity (v) as a function of r for different values of magnetic field B .

Figure 17 represents the escape velocity against radius r for different values of angular momentum L_z . From figure 17 we can say that the possibility for a particle to escape having large angular momentum is small. We have plotted escape velocity for different values of α in figure 18 and 18, $\alpha = 0$, correspond to S-BH (Schwarzschild Black Hole) and $\alpha = 1$ correspond to RN-BH.

In figure 18 we are comparing the escape velocity of a particle moving around the S-BH, RN-BH and MOG-BH. Note that the difference between the velocities is larger near the black hole (initially) and it becomes almost same away from the black hole. Therefore, we can conclude that the effect of the charge of black hole on the motion of the particle is large while it reduces as particle moves away from it. One can see that for large r escape velocity is same for all values of

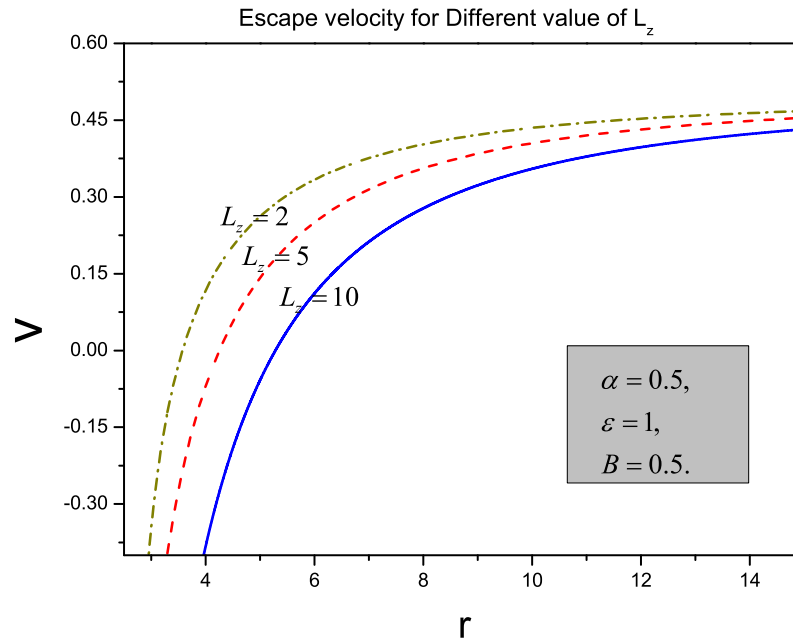


FIG. 17: Escape velocity (v) against r for different values of angular momentum ℓ .

α but for small r lesser value of α correspond to greater value of escape velocity and vice versa.

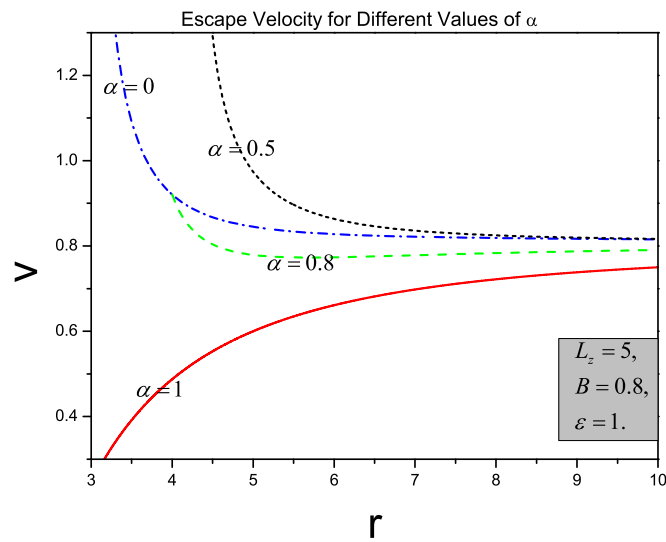


FIG. 18: Escape velocity (v) against r for different values of parameter α .

IX. SUMMARY AND CONCLUSION

We have investigated and compare the dynamics of a charged and a neutral particle in the vicinity of S-BH, RN-BH and MOG-BH. Geodesics of a neutral and a charged particle in the vicinity of a MOG-BH are shown in figures 5 and 6. We see that for a charged particle there are two boundaries on the geodesics, $r = r_h$ and $r = r_c$ unlike the formal case in which a neutral particle comes from infinity and goes back to infinity before reaching the horizon, $r = r_h$, of the BH. We discussed the effective potential behavior in details regarding the stability of the orbits of the particle. We further discussed the energy condition for the particle, when it will escape or its motion remains bound. Expressions for the escape velocity of the particle moving around MOG-BH and for magnetic field, present in the vicinity of BH due to plasma, is derived in this work. More importantly a comparison is done for effective potentials, obtained in the presence and absence of magnetic field. It is found that presence of magnetic field enhance the stability of the orbits of the moving particles, due to the presence of it width of stable region in contrast to which we obtained in the case when magnetic field is absent. We have also done the comparison of the effective potentials among the RN-BH, S-BH and MOG-BH. Further we studied the stability by Lyapunov exponent against magnetic field and a parameter α . We conclude that stability of orbits would increase due to the presence of vector field considered in MOG. We deduce that the particle have to face more repulsion to reach the singularity due to the presence of vector field as considered in MOG. But the presence of magnetic field might increase the attractive force. It is found that a particle with large value of angular momentum L_z would have greater possibility to reside in the stable orbits in comparison with a particle with lesser value of it. Therefore, escape velocity is less correspond to particle with large value of L_z . Effects of magnetic field and parameter α on escape velocity are also investigated graphically. It is concluded that presence of magnetic field might provide sufficient energy to particle to escape easily from the surrounding of BH.

Acknowledgment

The authors would like to thank both referees and Lim Yen-Kheng for very useful comments to improve this paper.

-
- [1] C. Deffayet, Phys. Lett. B **502** (2001) 199;
 J. S. Alcaniz, Phys. Rev. D **65**, 123514 (2002);
 S. M. Carroll, V. Duvvuri, M. Trodden and M. Turner, Phys. Rev. D **70**, 043528(2004);
 S. Nojiri and S. D. Odintsov, Phys. Lett. B **576** (2003) 5;
 K. Atazadeh and H. R. Sepangi, Int. J. Mod. Phys. D **16**, 687 (2007);
 S. Nojiri, S. D. Odintsov and M. Sami, Phys. Rev. D **74**, 046004 (2006);
 I. Navarro and K. Van Acoleyen, J. Cosmol. Astropart. Phys. **0603**, 008 (2006);
 S. Capozziello, Int. J. Mod. Phys. D **11**, (2002) 483;
 S. Nojiri and S. D. Odintsov, Phys.Rev. D **68**, 123512 (2003).
- [2] S. Capozziello, M. De Laurentis, Phys. Rept. **509**, 167 (2011);
 S. Nojiri, S. D. Odintsov, Phys. Rept. **505**, 59 (2011).
- [3] G. Magnano, M. Ferraris, and M. Francaviglia, Gen. Rel. Grav. **19**, 465 (1987).
- [4] J. D. Barrow, and A. C. Ottewill, J. Phys. A: Math. Gen. **16**, 2757 (1983).
- [5] N. D. Birrell and P. C. W. Davies, Quantum Fields in Curved Space (Cambridge University Press, 1982).
- [6] G. Vilkovisky, Class. Quantum Grav. **9**, 895 (1992).
- [7] A. A. Starobinsky, Phys. Lett. B **91**, 99 (1980).
- [8] D. La, and P. J. Steinhardt, Phys. Rev. Lett. **62**, 376 (1989);
 D. La , P. J. Steinhardt and E. W. Bertschinger, Phys. Lett. B **231**, 231 (1989).
- [9] J. W. Moffat, Eur. Phys. J. C **75**, 175 (2015).
- [10] A. Zakria, M. Jamil, JHEP **05**, 147 (2015);
 I. Hussain, M. Jamil, B. Majeed, Int. J. Theor. Phys. **54**, 1567 (2015).
- [11] T. Harada and M. Kimura, Class. Quantum Grav. **31**, 243001 (2014).
- [12] M. A. Podurets, Astr. Zh. **41**, 1090 (1964) (English translation in Sovet Astr.- AJ, **8**,868 (1965)).
- [13] W. L. Ames and K. S. Throne, J. Astrophys. **151**, 659 (1968).
- [14] C. V. Borm, M. Spaans, Astron. Astrophys. **553**, L9(2013).
- [15] J. C. Mckinney, R. Narayan, Mon. Not. Roy. Astron. Soc. **375**, 523 (2007).
- [16] P. B. Dobbie, Z. Kuncic, G. V. Bicknell, and R. Salmeron. Proceedings of IAU Symposium 259: Cosmic Magnetic Fields: From Planets, To Stars and Galaxies (Tenerife, 2008).
- [17] R. Znajek, Nature **262**, 270 (1976).

- [18] V. P. Frolov and P. Krtous, *Phys. Rev. D* **83**, 024016 (2011).
- [19] R. D. Blandford, R. L. Znajek, *Mon. Not. Roy. Astron. Soc.* **179**, 433 (1977).
- [20] S. Koide, K. Shibata, T. Kudoh, and D. I. Meier, *Science* **295**, 1688(2002).
- [21] S. Kide, *Phys. Rev. D* **67**, 104010 (2003).
- [22] M. Jamil, A. Qadir, *Gen. Rel. Grav.* **43**, 1069 (2011);
B. Nayak, M. Jamil, *Phys. Lett. B* **709**, 118 (2012);
M. Jamil, D. Momeni, K. Bamba, R. Myrzakulov, *Int. J. Mod. Phys D* **21**, 1250065(2012);
M. Jamil, M. Akbar, *Gen. Rel. Grav.* **43**, 1061 (2011).
- [23] A. M. A. Zahrani, V. P. Frolov, A. A. Shoom, *Phys. Rev. D* **87**, 084043 (2013).
- [24] S. Hussain, I. Hussain, M. Jamil, *Eur. Phys. J. C* **74**, 3210 (2014).
- [25] M. Jamil, S. Hussain, B. Majeed, *Eur. Phys. J. C* **75**, 24 (2015).
- [26] J. W. Moffat, *JCAP* **0603**, 3004 (2006).
- [27] J.W. Moffat, arXiv:1101.1935 [astro-ph.CO]; J. W. Moffat, V. T. Toth, arXiv:1104.2957 [astro-ph.CO];
ibid, arXiv:1005.2685 [gr-qc]; ibid, *AIP Conf. Proc.* **1241**, 1066 (2010).
- [28] J. W. Moffat, V. T. Toth, *Mon. Not. Roy. Astron. Soc.* **397**, 1885 (2009).
- [29] V. Frolov, *The Galactic Black Hole* (Editors: H. Falcke, F. H. Hehl), IoP (2003).
- [30] V. P. Frolov, *Phys. Rev. D* **85**, 024020 (2012).
- [31] G. Nordstorm, *Proc. Kon. Ned. Akad. Wet.* **29**, 1238 (1918).
- [32] H. Reissner, *Ann. Physik*, **50**, 106 (1916).
- [33] R. P. Kerr, *Phys. Rev. Lett.* **11**, 237 (1963).
- [34] T. Igata, T. Koike, and H. Ishihara, *Phys. Rev. D* **83**, 065027 (2011).
- [35] L. D. Landau and E. M. Lifshitz, *The Classical Theory of Fields* (Pergamon Press, Oxford, 1975).
- [36] S. Chandrasekher, *The Mathematical Theory of Black Holes* (Oxford University Press, 1983).
- [37] B. Punsky, *Black Hole Gravitohydrodynamics* (Springer-Verlag, Berlin, 2001).
- [38] D. X. Wang , K. Xiao, W. -H. Lei, *MNRAS* **335**, 655 (2002).
- [39] Wang D.-X., Ma R.-Y., Lei W.-H., Yao G.-Z., *ApJ* **595**, 109 (2003).
- [40] Zhang W.M., Lu Y., Zhang S. N, *Chin. J. Astron. Astrophys.*, **5**, 347 (2005),.
- [41] M. Yu. Piotrovich, N. A. Silant, Yu.N. Gnedin, T.M. Natsvlishvili, arXiv:1002.4948v1
- [42] R. M. Wald, *Phys. Rev. D* **10**, 1680 (1974).
- [43] A. A. Abdujabbarov, B. J. Ahmedov and N.B. Jurayeva, *Phys. Rev. D* **87**, 064042 (2013).
- [44] A. N. Aliev and N. Ozdemir, *Mon. Not. Roy. Astron. Soc.* **336**, 241 (1978).
- [45] H. Q. Hong, C. J. Hua, W. Y. Jiu *Chin. Phys. Lett.* **31**, 060402 (2014).
- [46] S. Fernando, arXiv:1202.1502v4
- [47] V. Cardoso, A. S. Miranda, E. Berti, H. Witek and V. T. Zanchin, *Phy. Rev.* **D79**, 064016 (2009).
- [48] R. Emparan and R. C. Myers, *JHEP* **0309**, 025 (2003) arXiv: hep-th/0308056.
- [49] V. P. Frolov and A. A. Shoom, *Phys. Rev. D* **82**, 084034 (2010).